A NUMERICAL STUDY OF NATURAL CONVECTION AND RADIATION INTERACTION IN VERTICAL CIRCULAR PIN

E. Khoshravan and G. Soleimani

Department of Mechanical Engineering
Univercity of Tabriz
Tabriz, Iran

Abstract A numerical finite difference study has been carried out for two dimensional radiation-natural convection interaction phenomena in a vertical circular pin located at a non-participating (i.e. transparent) fluid. The coupled conservation equations in boundary layer (continuity, momentum, and energy equations) and pin energy equation are solved simultaneously using modified box method and fully implicit finite difference scheme. The effect of three major parameters on pin temperature distribution, velocity and temperature profile at boundary layer, local heat transfer coefficient, and local heat flux are examined in detail. These parameters are radiation-conduction parameter. Also the surface heat transfer coefficient increases with increasing radiative interaction.

Key Words Natural Convection, Radiation, Heat Transfer, Finite Difference, Circular Pin

چکیده در این مقاله تاثیر متقابل تابش و همرفت آزاد در میله استوانه ای که بطور قائم در سیال غیر سهیم (شفاف) قرار گرفته است با روش اختلاف محدود بررسی شده است. معادلات بقا در لایه مرزی (معادله پیوستگی، معادله ممنتوم و معادله انرژی) و معادله انرژی در میله بطور همزمان با استفاده از روش جعبه ای اصلاح شده و روش اختلاف محدود ضمنی حل شده است. تاثیر سه پارامتر مهم (پارامتر همرفت-رسانش، پارامتر تابش-رسانش و عدد پرانتل) بر روی توزیع دما در میله، توزیع سرعت و دما در لایه مرزی، ضریب انتقال حرارت محلی و شار گرمای محلی بطور مفصل مورد مطالعه واقع شده است. نتایج نشان می دهد اندازه پارامتر همرفت-رسانش تاثیر زیادی بر روی شار گرمای سطح میله داشته و نیز افزایش پارامتر تابش-رسانش باعث افزایش ضریب انتقال حرارت می شود.

INTRODUCTION

Recently, the problem of heat tranfer in a fin has received considerable attention due to its extensive applications such as in cooling systems. In the conventional approach to determine the heat transfer characteristics of fins, the fin heat conduction equation is solved using a literature-given value of the convective heat transfer coefficient that is assumed to be uniform along the fin surface. This approach leads to uncertain results because, in general, the heat transfer coefficient varies along the fin surface. Also the available literature information may not correspond to the actual fluid flow and/or thermal boundary conditions for the fin. Research in conjugate convection-conduction heat transfer in fins has been presented by investigators. Sparrow and Acharya [1] and Sparrow and Chyu [2] analyzed conjugate convection-conduction problems for a vertical plate fin using finte difference method. Investigation of conjugate convection-conduction heat transfer without thermal radiation effects in circular pins was presented by Huang et al [3] and Huang and Chen [4]. They concluded that convective fin analysis based on a uniform heat transfer coefficient value gave good prediction for overall heat transfer rate of the fin, yet could not accurately predict local heat flux. An alternative to the aforementioned procedure is to

simultaneously solve the conduction problem for the fin and the convective heat transfer problem for the flowing fluid with thermal radiation interaction. In natural convection, when buoyancy and thermal radiation effects are of the same importance, a separate calculation of radiation and convection and their superposition without considering the interaction between them can lead to erratic results, because the presence of thermal radiation alters the temperature and velocity distributions in the boundary layer [5-9]. Therefore, in such a situation, heat transfer due to buoyancy and radiation should be solved for simultaneously. Combined natural convection and radiation heat transfer from a vertical plate fin, which is situated in nonparticipating and participating media, was presented by Sarma and Subrabmanyam [10] and Hsu and Tasi [11] respectively. The present paper is concerned with circular pin which transfers heat to a surrounding fluid by natural convection and radiation. The problem is investigated numerically by a fully implicit finite difference method and modified box scheme with two types of grid sapcing. The objective of this article is to present numerical results in terms of the distribution of the local heat transfer coefficient, and heat flux. The solutions are governed by two parameters, one of which will be termed the radiation-conduction parameter and the other is the convection-conduction parameter. The effects of radiation-conduction and convection-conduction parameters on themal behavior of the boundary layer are also discussed. Values of these parameters were selected to cover the practically realistic operating conditions.

ANALYSIS

Consider a vertical circular pin of radius r_o, with base temperature T_o which is situated in a quiescent environment having temperature T_∞. Here, we assume $T_\infty < T_o$, which means that the flow moves upward and the gravity g acts downward in the opposite direction to the flow. The coordinate system is illustrated in the inset of Figure 1.

The complete mathematical formulation of simultaneous convection and radiation includes the convection and the radiation parts. For transparent fluids considered here, the presence of thermal radiation dose not alter the standard equations of motion and energy; hence by employing the Boussinesq approximation for the fluid properties, the natural convective boundary layer equations are [4]

$$\frac{\partial (ru)}{\partial x} + \frac{\partial (rv)}{\partial r} = 0 \tag{1}$$

$$u\frac{\partial u}{\partial x} + v\frac{\partial u}{\partial r} = g\beta (T - T_\infty) + \frac{\nu}{r}\frac{\partial}{\partial r}\left(r\frac{\partial u}{\partial r}\right) \tag{2}$$

$$u\frac{\partial T}{\partial x} + v\frac{\partial T}{\partial r} = \frac{\alpha}{r}\frac{\partial}{\partial r}\left(r\frac{\partial T}{\partial r}\right) \tag{3}$$

where u and v are the streamwise and radial velocity components, respectively, T is the fluid temperature, α is the thermal diffusivity , and υ is the kinematic viscosity. The system of equations (1-3) is subject to the following boundary conditions:

$$\begin{aligned} &r = r_0,\ 0 < x < L \quad && u = v = 0, && T = T_w(x) \\ &r \to \infty,\ 0 < x < L \quad && u \to 0, && T = \to T_\infty \end{aligned} \tag{4}$$

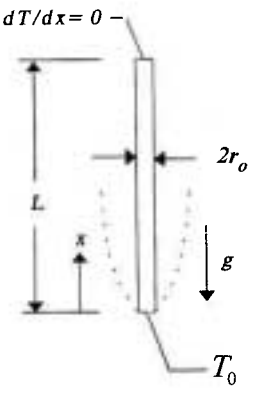

Figure 1. System configuration and coordinate system.

$x = 0, r > r_o \qquad u = 0, \qquad T = T_\infty$

The energy equation for the circular thin pin with a one-dimensional model for the temperature distribution along the longitudinal direction is

$$\frac{d^2 T_f(x)}{dx^2} - \frac{2 h_t(x)}{k_f r_0} (T_f(x) - T_\infty) = 0 \qquad (5)$$

where k_f is the pin thermal conductivity, $T_f(x)$ is the pin temperature, and $h_t(x)$ is the local combined convection-radiation heat transfer coefficient. The associated boundary conditions of the energy equation of the circular pin are

$$x = 0 \qquad T_f(x) = T_o \qquad (6a)$$

$$x = L \qquad \frac{dT_f(x)}{dx} = 0 \qquad (6b)$$

Since the circular pin considered is relatively long compared to its diameter, the amount of heat which passes from the tip of the circular pin to the fluid is negligible. Therefore, the assumption of an adiabatic tip is justified. The energy transport from the pin wall to the ambient in the presence of thermal radiation depends on two related factors: the fluid temperature gradiant at the pin wall and the rate of radiative heat exchange. Hence, the wall heat flux, $q_w(x)$, at the pin surface can be expressed as

$$q_w(x) = q_{con}(x) + q_{rad}(x) \qquad (7a)$$

$$q_w(x) = h_t(x) (T_f(x) - T_\infty) \qquad (7b)$$

$$q_{con}(x) = - k \left.\frac{\partial T}{\partial r}\right|_{r = r_0} \qquad (7c)$$

$$q_{rad}(x) = \varepsilon \sigma \left(T_f^4(x) - T_\infty^4\right) \qquad (7d)$$

where $q_{con}(x)$ and $q_{rad}(x)$ represent the wall heat flux due to convection and radiation, respectively. Of particular interest is the thermal coupling between the circular pin and the convective boundary layer. The basic coupling is expressed by the requirement that the pin and fluid temperatures and heat fluxes be continuous for all x at the pin-fluid interface, that is,

$$T_f(x) = T_w(x) \qquad (8a)$$

$$h_t(x) (T_f(x) - T_\infty) = - k \left.\frac{\partial T}{\partial r}\right|_{r = r_0} + \varepsilon\sigma \left(T_f^4(x) - T_\infty^4\right) \qquad (8b)$$

Therefore the pin energy equation can be written as:

$$\frac{d^2 T_f(x)}{dx^2} + \frac{2k}{k_f r_0} \left.\frac{\partial T}{\partial r}\right|_{r = r_0} - \frac{2 \varepsilon\sigma}{k_f r_0} \left(T_f^4(x) - T_\infty^4\right) = 0 \qquad (9)$$

Equations 1-3 and 9 can reduced to a system of dimensionless equations by introducing the following definitions:

$$X = \frac{x}{L} \quad , \quad R = \frac{r}{L} Gr_L^{1/4}$$

$$U = \frac{u L}{\nu} Gr_L^{-1/2} \quad , \quad V = \frac{v L}{\nu} Gr_L^{-1/4} \qquad (10)$$

$$\theta = \frac{T - T_\infty}{T_0 - T_\infty} \quad , \quad \theta_f = \frac{T - T_\infty}{T_0 - T_\infty}$$

where the Grashof number Gr_L is defined as

$$Gr_L = \frac{g \beta (T_0 - T_\infty) L^3}{\nu^2}$$

Introducing non-dimensional parameters (10) into Equations 1-3 and 9 results in:

$$\frac{\partial (RU)}{\partial X} + \frac{\partial (RV)}{\partial R} = 0 \qquad (11)$$

$$U \frac{\partial U}{\partial X} + V \frac{\partial U}{\partial R} = \theta + \frac{1}{R} \frac{\partial}{\partial R} \left(R \frac{\partial U}{\partial R}\right) \qquad (12)$$

$$U \frac{\partial \theta}{\partial X} + V \frac{\partial \theta}{\partial R} = \frac{1}{Pr} \frac{1}{R} \frac{\partial}{\partial R} \left(R \frac{\partial \theta}{\partial R}\right) \qquad (13)$$

$$\frac{d^2\theta_f}{dX^2} + 2\psi_C \left.\frac{\partial \theta}{\partial R}\right|_{R=R_0} - \frac{2\psi_R}{\psi_T}\left[(1+\theta_f\psi_T)^4 - 1\right] = 0 \quad (14)$$

where Pr = υ/α is the Prandtl number , $\psi_R = \varepsilon\sigma T_\infty^3 L^2/(k_f r_o)$ the radiation-conduction parameter, $\psi_C = KL\,G\,r_L^{1/4}/(k_f r_o)$, the convection-conduction parameter, and $\psi_T = (T_0 - T_\infty)/T_\infty$ the temperature ratio. The transformed boundary conditions are

$R = R_0$	U=V=0,	$\theta=\theta_f$
$R\to\infty$	U=0,	$\theta=0$
$X = 0, R>R_0$	U=0,	$\theta=0$

(15)

The corresponding conditions for the pin are

$$X=0 \qquad q_f = 1 \quad (16a)$$

$$X=L \qquad \frac{d\theta_f}{dX} = 0 \quad (16b)$$

In the foregoing equations, the standard symbols are defined in the nomenclature and the transverse curvature parameter R_0 and dimensionless local combined convection-radiation heat transfer coefficient is given by

$$R_0 = \frac{r_0}{L} G\, r_L^{1/4} \quad (17)$$

$$\frac{h_0(x)\,L}{K\,G\,r_L^{1/4}} = -\frac{1}{\theta_f}\left.\frac{\partial\theta}{\partial R}\right|_{R=R_0} + \frac{\psi_R}{\psi_C\psi_T}\frac{1}{\theta_f}\left[(1+\psi_T\theta_f)^4 - 1\right] \quad (18)$$

the local heat transfer coefficient is defined as

$$h_t(x) = h_{con}(x) + h_{rad}(x) \quad (19)$$

$$h_{con}(x) = \frac{-K}{L\,Gr_L^{1/4}}\frac{1}{\theta_f}\left.\frac{\partial\theta}{\partial R}\right|_{R=R_0} \quad (20)$$

$$h_{rad}(x) = \frac{\psi_R}{\psi_C\psi_T}\frac{k\,Gr_L^{1/4}}{L\,\theta_f}\left[(1+\psi_T\theta_f)^4 - 1\right] \quad (21)$$

and the local heat flux can be taken as

$$\frac{q_w(x)\,L}{k\,Gr_L^{1/4}(T_0 - T_\infty)} = -\left.\frac{\partial\theta}{\partial R}\right|_{R=R_0} + \frac{\psi_R}{\psi_C\psi_T}\left[(1+\psi_T\theta_f)^4 - 1\right] \quad (22)$$

NUMERICAL PROCEDURE

The governing Equatins 11-14 are discretized by fully implicit finite difference procedure based on modified box scheme. This implicit finite difference scheme is a marching method that begins at the pin root (X = 0) and proceeds step by step until the pin top (X=1) is reached. Together with the boundary conditions (15-16) approximate solutions are obtained by Newton-Raphson iterative method. To ensure high accuracy, a step-size study was performed prior to the initiation of the main calculation. The final grid pattern encompassed 60 grid points in the cross-stream (R) direction and 40 grid points in the streamwise (X) direction. There was a denser concentration of grid points near the leading edge (small X) to accommodate the initial rapid growth of the boundary layer. In addition, at all X, the grid points were more densely concentrated near the pin surface. For grid spacing, a constant ratio between two adjacent increments was used:

$$\frac{\Delta R_{J+1}}{\Delta R_J} = k_1 \quad , \quad \frac{\Delta X_{n+1}}{\Delta X_n} = k_2$$

where j and n are the grid location in R direction and marching step respectively. The accuracy (and occasionally the stability) of modified box scheme appears sensitive to the value of k_1 and k_2 being used. In this study, the suitable values for k_1 and k_2 are 1.038 and 1.042 respectively. At each marching step, convergence is assumed when the following convergence criterion is satisfied:

$$\frac{\|\Phi_z - \Phi_{z-1}\|_\infty}{\|\Phi_z\|_\infty} \leq 10^{-4} \quad \text{for all } \Phi$$

where Φ refers to any dependent variable (θ, U, V), z stands for the z th iteration, and $\| \|_\infty$ is the infinite norm. It is found in the separate computation that the difference in results obtained by using fully implicit finite difference scheme with 90×100 equally spaced grid points, and modified box method with 60×40 unequally spaced grid points are always less than 3 percent. Also the computation time for the modified box method is almost half of the computation time needed to preform the fully implicit scheme. When convergence temperature field is reached, the local dimensionless combined convection-radiation heat transfer coefficient and heat flux can be calculated from Equations 18 and 22 respectively.

RESULTS AND DISCUSSION

Numerical computations have been carried out for $\Delta R_1 = 0.075$, $\Delta X_1 = 0.01$, Pr = 0.72 and 1, radiation-conduction parameter (ψ_R)=0, 0.05 and 0.1, covection-conduction parameter (ψ_C)=0.2, 1 and 1.5, temperature ratio (ψ_T) = 3 and transverse curvature parameter R_0 = 1.25. Plots are presented for velocity and temperature distribution in the boundary layer, variations of local heat transfer coefficient and local heat flux, and temperature distribution in the pin

The radiation-conduction parameter ψ_R is defined as the ratio of radiation effect to conduction effect. The effect of radiation is getting strong as the ψ_R increases. Figure 2 shows the effects of ψ_R on the dimensionless axial velocity distribution at different axial coordinates. In non-participating media, with increasing ψ_R, the axial velocity decreases. This implies that the presence of radiation effects tend to reduce the effect of buoyancy. Figure 3 represents the effects of convection-conduction parameter ψ_C on axial velocity distribution. The greater value of ψ_C indicates the smaller pin thermal conductivity. Hence, at the higher value of ψ_C, temperature at any location along the pin reduces, and the buoyancy effect decreases. In other words, when ψ_C is increased, the peak of velocity profile is lowered. The effect of Prandtl number on the velocity and temperature

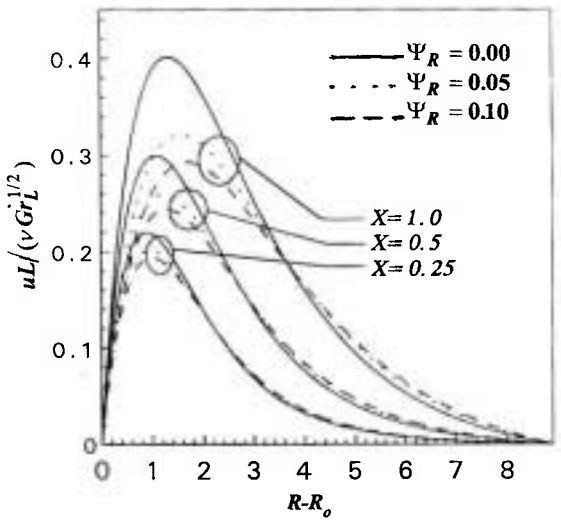

Figure 2. Effect of radiation-conduction parameter on dimentionless velocity profile in boundary layer, ψ_C=1., ψ_T = 3., Pr = 0.72.

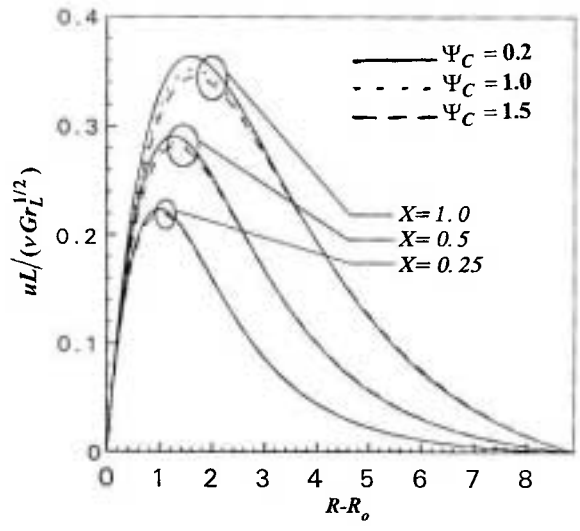

Figure 3. Effect of convection-conduction parameter on dimensionless velocity profile in boundary layer, ψ_R = 0.05, ψ_T = 3., Pr= 0.72.

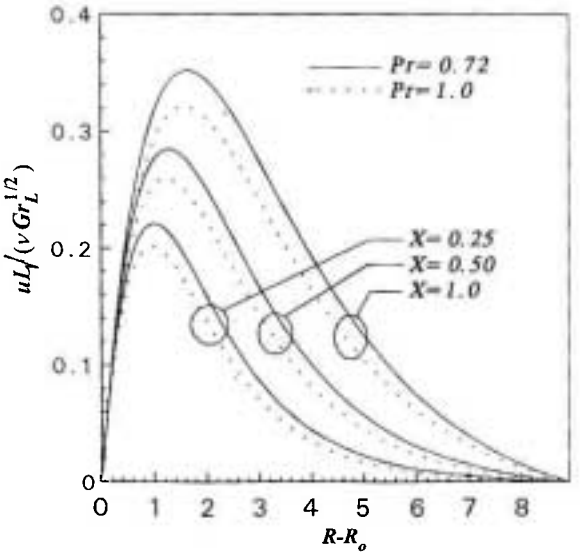

Figure 4. Effect of Prandtl number on dimensionless velocity profile in boundary layer, $\psi_R = 0.05$, $\psi_C = 1.0$, $\psi_T = 3$.

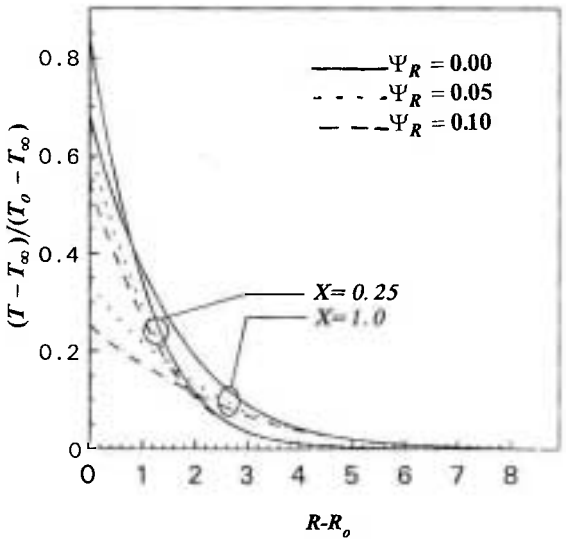

Figure 6. Effect of adiation-conduction parameter on dimensionless temperatuer profile in boundary layer, $\psi_C = 1.$, $\psi_T = 3.$, Pr = 0.72.

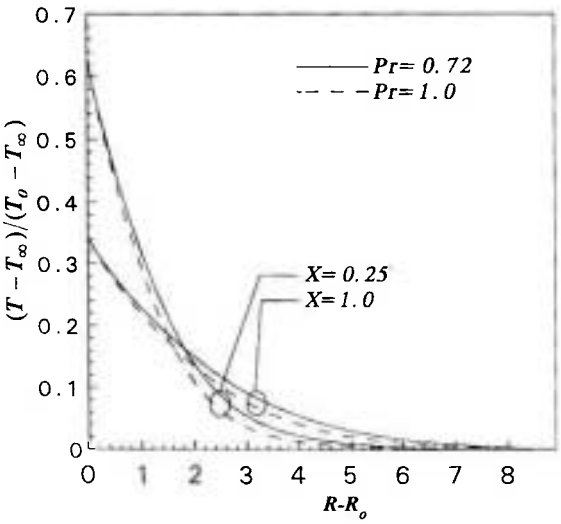

Figure 5. Effect of prandtl number on dimensionless temperatue profile in boundary layer, = 0.05, =1., = 3.

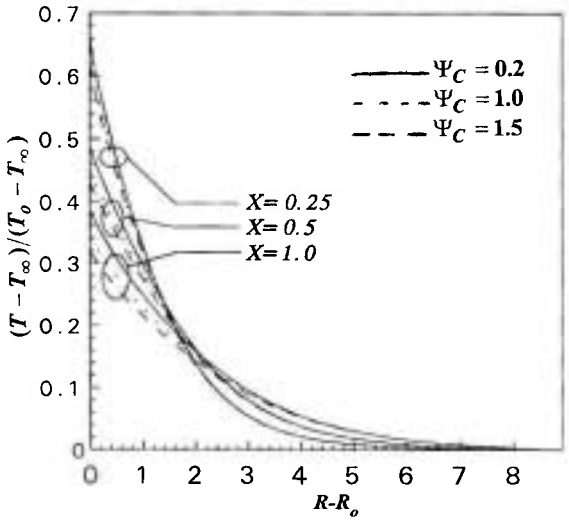

Figure 7. Effect of convection-conduction parameter on dimensionless temperature profile in boundary layer, $\psi_R = 0.5$, $\psi_T = 3.$, Pr = 0.72.

profiles are shown in Figures 4 and 5. An increase in Pr is found to cause a decrease in thermal boundary layer thickness and an increase in the absolute value of the temperature gradient at the surface. It was also found that the dimensionless maximum velocity and the velocity gradient at the surface decrease with increasing Pr, indicating the effect of greater viscous forces. The location of this maximum value is found to shift to higher R as Pr is decreased. The velocity boundary layer thickness is also found to increase as Pr is switched to lower values [12, 13]. Figure 6 demonstrates the effects of the radiation-conduction parameter ψ_R, on dimensionless temperature distribution in boundary layer at different axial locations. It is clearly shown that as thermal radiation

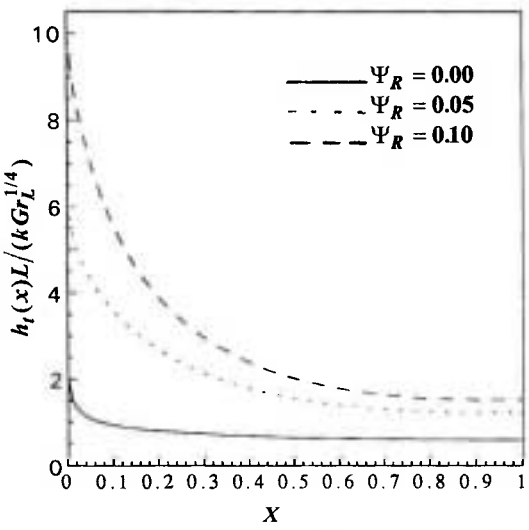

Figure 8. Effect of radiation-conduction parameter on dimensionless local heat transfer coefficient, ψ_C=1., ψ_T=3., Pr=1.

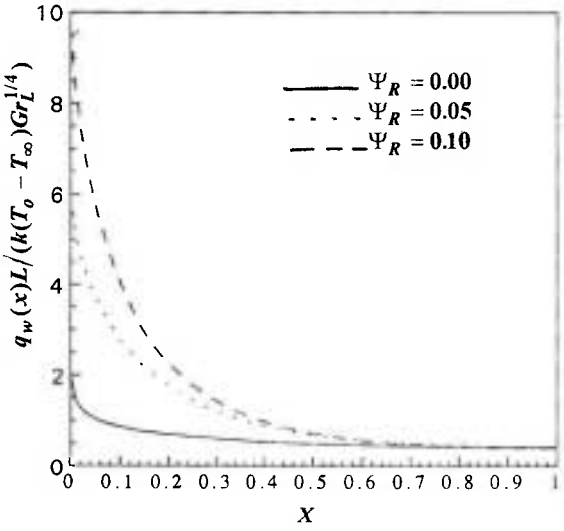

Figure 10. Effect of radiaion-conduction parameter on dimensionless local heat flux, ψ_C=1., ψ_T=3., Pr=1.

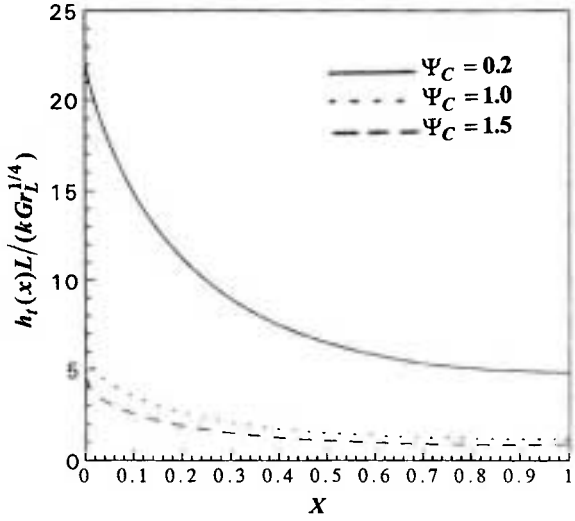

Figure 9. Effect of convection-conduction parameter on dimonsionless local heat transfer coefficient, ψ_R=0.05, ψ_T=3., Pr=1.

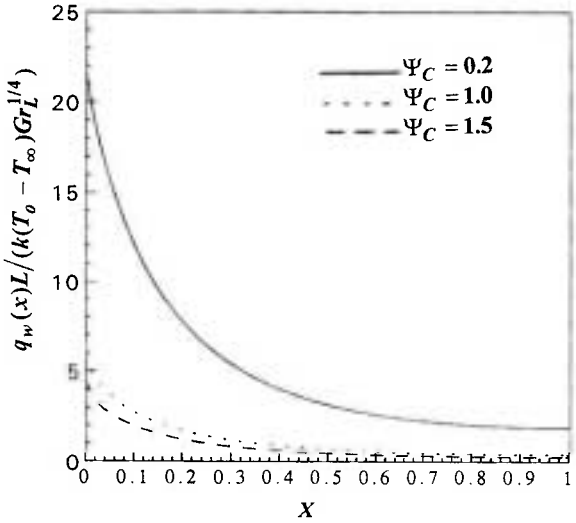

Figure 11. Effect of convection-conduction parameter on dimensionless local heat flux, ψ_R = 0.05, ψ_T=3., Pr=1.

intensifies (i.e. the value of ψ_R increases), heat flux from the surface increases, causing the wall temperature and temperature gradient in boundary layer to decrease. Figure 7 illustrates the distribution of temperature in boundary layer as a function of convection-conduction parameter ψ_C for fixed values of Pr, ψ_R, and ψ_T. The greater value of ψ_C indicates the smaller pin conductance. Therefore, the increasing values of ψ_C give the decreasing pin temperature and cause the temperature gradient in the fluid at the boundary layer to decrease. The variation of local heat transfer coefficients and local heat flux along the length of the pin for different values of parameter ψ_R and ψ_C are depicted in Figures 8, 9, 10 and 11. It is evident from Figures 8 and 10 that radiation considerably enhances the local heat transfer

coefficient and local heat flux. Figures 9 and 11 indicate that an increase in convection-conduction parameter (decrease in pin conductance), causes a drop in the local heat transfer coefficient and local heat flux. This is due to the increasing temperature gradient in the pin. Since the temperature in the vicinity of pin root is higher than that of other location on the pin, it is seen that in the region near the root of the pin, heat transfer coefficient and heat flux increase. The effects of the radiation-conduction parameter and convection-conduction parameter on the pin temperature distribution are shown clearly in Figures 12 and 13 respectively. In Figure 12, the influence of the radiation-conduction parameter on the variation of temperature gradient at the pin root (X = 0) is significantly large. For the larger value of ψ_R, thermal radiation becomes the dominant mode of heat transfer, causing the surface temperature to decrease and the temperature gradient at the pin length to increase. Therefore, when radiation component goes up, the local temperature along the pin wall will be less than those observed for the case of negligible radiation from the pin surface. From the definition of ψ_C, decreasing values of ψ_C are indicative of higher pin conductivity, leading to a reduction in the temperature profile along the pin (Figure 13). To verify the accuracy of the present work, the system can be reduced to a case with zero thermal radiation exchange. Figures 14 and 15 show the results of M. J. Huang et al [4] and present work for dimensionless pin temperature distribution, dimensionless heat tranfer coefficient, and dimensionless heat flux. Comparison of these curves shows an agreement between the results of M. J. Huang et al and those of the present work.

CONCLUSION

The interaction of thermal radiation with conduction and convection for vertical circular pin has been investigated. The governing equations are solved by modified box method and fully implicit finite difference technique. It was found that the computation time for the modified box method (with 60 ×40 unequally spaced grid points) is almost half of the computation time needed to perform the

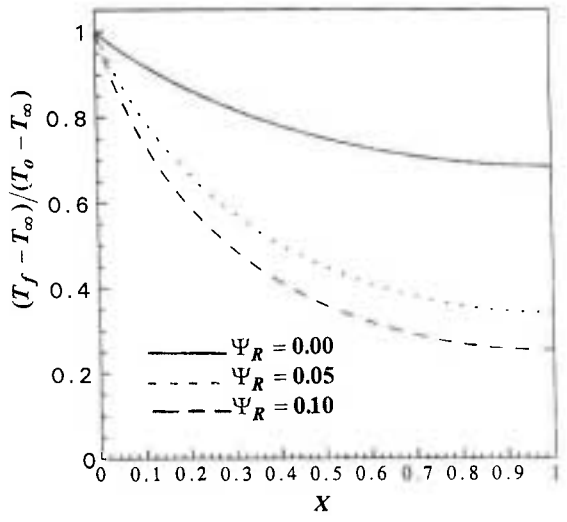

Figure 12. Effect of radia on-conduction parameter on dimensionless pin temperatue distribuion, , ψ_C=1., ψ_T=3., Pr = 1.

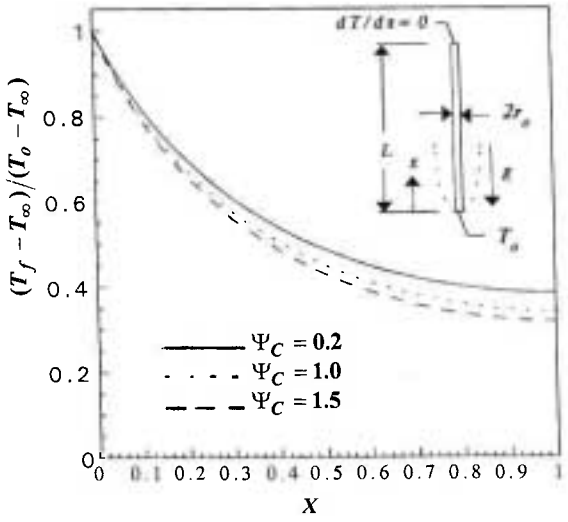

Figure 13. Effect of convection-conduction parameter on dimensionless Pin temperatue distribution, ψ_R = 0.05, ψ_T = 3., Pr = 0.72.

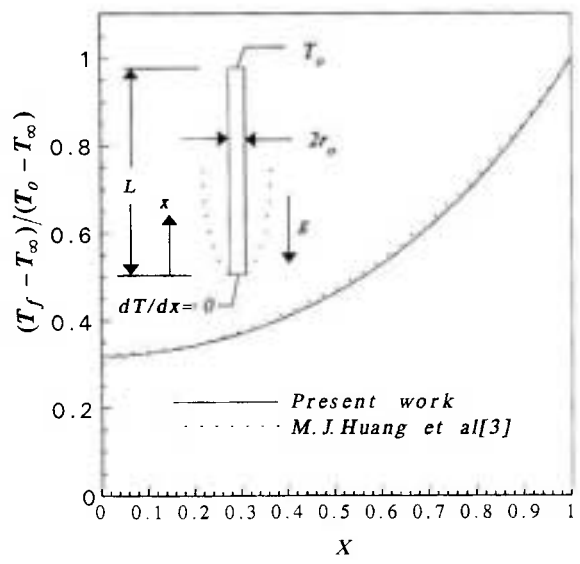

Figure 14. Dimensionless temperatue distrubtion of circular pin, $\psi_R = 0.0$, $\psi_C = 2.5$, Pr=1.

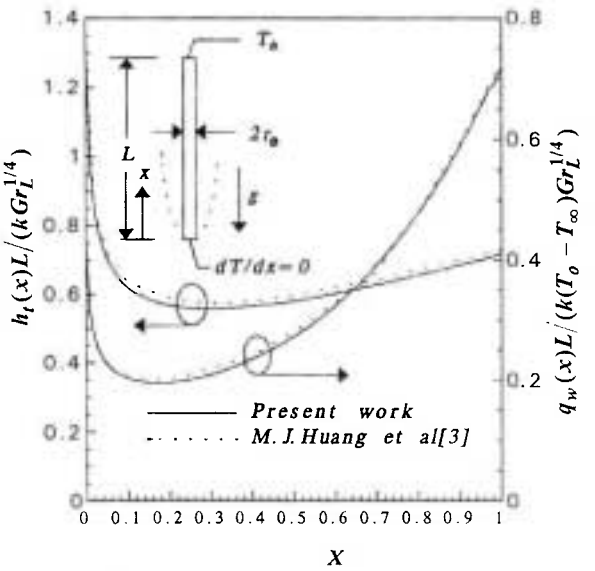

Figure 15. Dimensionless local heat transfer coefficient and local heat flux, $\psi_R = 0.0$, $\psi_C = 2.5$., Pr = 0.72.

fully implicit scheme (with 90×100 equally spaced grid points). The effects of different physical parameters, such as radiation-conduction parameter ψ_R, convection-conduction parameter ψ_C, and Prandtl number are systematically studied. The results presented here have shown that the radiation highly activates heat transfer characteristics. In non-participating media, the thicknesses of the velocity and thermal boundary layers and maximum velocity of the fluid decrease as the radiation heat transfer becomes more dominant. With the increase in the radiation-conduction parameter ψ_R, the energy exchange between the pin wall and surrounding medium is enhanced as a result of greater radiation effect. Temperature distribution in the pin is influenced by the radiation effect. The numercial results show that the surface heat flux is also affected dominantly by the convection-conduction parameter. A pin with a small convection-conduction parameter reveals higher surface temperature and surface heat flux.

NOMENCLATURE

g	acceleration of gravity
Gr	Grashof number
h	local heat transfer coefficient
$h_{con}(x)$	local convective heat transfer coefficient
$h_{rad}(x)$	local radiative heat transfer coefficient
k_f	thermal conductivity of pin
k	fluid thermal conductivity
L	pin length
Pr	prandtl number
$q_w(x)$	local wall heat flux
$q_{con}(x)$	local convective heat flux
$q_{rad}(x)$	local radiative heat flux
r_0	radious of pin
r	radial coordinate
R	dimensionless radial coordinate
R_0	transvers curvature parameter
T	temperature of fluid
T_f	temperature of pin
T_0	root temperature of pin
T_w	pin wall temperature
T_∞	ambient temperatue
u	axial velocity
U	dimensionless axial velocity
v	radial velocity